



Analytical Characterisation of Material Corrosion by Biofilms

Yen T. H. Dang¹ · Aoife Power² · Daniel Cozzolino³ · Khuong Ba Dinh^{4,5} · Binh Son Ha⁶ · Adam Kolobaric⁸ · Jitraporn Vongsivut⁷ · Vi Khanh Truong^{1,8} · James Chapman⁸ 

Received: 1 December 2021 / Revised: 11 January 2022 / Accepted: 14 February 2022 / Published online: 6 March 2022
© The Author(s) 2022

Abstract

Almost every abiotic surface of a material is readily colonised by bacteria, algae, and fungi, contributing to the degradation processes of materials. Both biocorrosion and microbially influenced corrosion (MIC) refer to the interaction of microbial cells and their metabolic products, such as exopolymeric substances (EPS), with an abiotic surface. Therefore, biofouling and biodeterioration of manufactured goods have economic and environmental ramifications for the user to tackle or remove the issue. While MIC is typically applied to metallic materials, newly developed and evolving materials frequently succumb to the effects of corrosion, resulting in a range of chemical reactions and transport mechanisms occurring in the material. Recent research on biocorrosion and biofouling of conventional and novel materials is discussed in this paper, showcasing the current knowledge regarding microbial and material interactions that contribute to biocorrosion and biofouling, including biofilms, anaerobic and aerobic environments, microbial assault, and the various roles microorganisms' play. Additionally, we show the latest analytical techniques used to characterise and identify MIC on materials using a borescope, thermal imaging, Fourier transform infrared (FTIR), atomic force microscopy (AFM), scanning electron microscopy (SEM), X-ray photoelectron microscopy (XPS), X-ray diffraction (XRD), optical and epifluorescence microscopy, electrochemical impedance spectroscopy, and mass spectrometry, and chemometrics.

Keywords Biocorrosion · Biofilm

1 Introduction

The processes by which microbial organisms accelerate the corrosion rate of materials by microorganisms are generally referred to as biocorrosion, or more specifically, microbially induced corrosion (MIC) [1–3]. Materials that undergo microbial colonisation typically undergo chemical reactions, which are cathodic or anodic, or the establishment of differential oxygen concentration cells in a localised electrolytic environment. The economic cost of biocorrosion has been estimated to be at least 20% for material corrosion, amounting to a direct cost of 30–50 billion dollars per year globally [4]. For example, Michelangelo's statue of David underwent cleaning measures for the first time in 500 years and cost €165k [5]. The French have injected some \$250 million into a corrosion clean-up and protection of the Eiffel Tower in 1989 [6]. Thus, corrosion researchers and engineers have been interested in preventing biocorrosion for structural materials for decades. Numerous strategies, including biocides, cathodic protection, beneficial bacterial biofilms, and

✉ Vi Khanh Truong
vi.khanh.truong@rmit.edu.au

✉ James Chapman
james.chapman@rmit.edu.au

¹ Advanced Institute of Science and Technology, University of Da Nang, Da Nang, Vietnam

² Forensic Science Ireland, Dublin, Ireland

³ QAAFI, University of Queensland, St Lucia, QLD, Australia

⁴ Optical Sciences Centre, Swinburne University of Technology, Hawthorn, VIC 3122, Australia

⁵ International School, Vietnam National University, Hanoi, Vietnam

⁶ Department of Intensive Care Medicine and Clinical Toxicology, Danang Hospital, Da Nang, Vietnam

⁷ ANSTO-Australian Synchrotron, 800 Blackburn Road, Clayton, VIC 3168, Australia

⁸ School of Science, STEM College, RMIT University, Melbourne, VIC, Australia

protective coatings, have been proposed to combat biocorrosion [7].

MIC was first reported in the twentieth century by Gaines, R.H. (1910), who discussed the inherent corrosion causes of steel [8]. Further investigation was then intensified by von Wolzogen Kuhr and Van der Vlugt in 1934, in an attempt to interpret MIC using electrochemistry, whereby they proposed the theory of cathodic depolarisation to explain the role of sulphate-reducing bacteria (SRB) in the anaerobic MIC of steels [9].

Essentially, the cathodic depolarisation offered a classical mechanistic model for the explanation of MIC, where hydrogen is removed from the cathodic surface (iron), leading to the cathodic depolarisation where sulphate is reduced to sulphite [1–3, 10–13] (Fig. 1). The generation of hydroxide ions, which creates iron sulphide and hydroxide products, forces more iron to be dissolved at the site of the anode. The mechanistic approaches were only undertaken in the early 1960s; apart from these two efforts, publications are scarce. Any slight reference to MIC was made involving underground corrosion of iron structures by bacteria. An excellent review of these mechanistic behaviours has been recently published by [7].

2 Metal Corrosion

Corrosive processes for metals can occur in numerous forms, and classification of these processes can be addressed based on three primary factors [11, 14–16]:

- (i) *The mechanism of corrosion* involving the electrochemical effects or direct chemical surface reactions.
- (ii) *The appearance of the corroded surface* corrosion is either uniform, and the surface will corrode at the

same rate over the whole surface, or it can be localised, in which only small areas become affected.

- (iii) *The nature of the environment* the corrosion can be classified into two categories: ‘dry’ or ‘wet’.

Corrosion can be classed through physical appearance, either by the naked eye or microscopic techniques. The morphology of the attack forms the basis for some classification. Figure 1 illustrates a schematic classification of the common types of corrosion, which includes the non-biological (referring to corrosion) and biocorrosion (which involves the microorganisms). Non-biological corrosion refers to corrosion that does not involve microorganisms (i.e. bacteria, viruses, fungi).

Biological corrosion (i.e. biocorrosion) refers to corrosion that involves microorganisms. Biological corrosion occurs when microorganisms are present in a wet environment where they can feed on organic matter and produce acids.

Essentially, these corrosion types are evidently visible upon a surface of a material. However, some types of corrosion can fit into multiple categories, or some that are not so fitting into the category of corrosion. Each form of corrosion shall now be discussed in more detail. These points of discussion are always assumed to be in the aqueous state. However, corrosion can occur in other environments that cause the material to become *stressed*, for example, high temperatures, high pressures, and salinity. It is safe to assume that all materials are affected by uniform corrosion. Passive materials such as stainless steel (SS) or other high corrosion resisting alloys are normally subjected to a more localised form of attack. Metals can resist corrosion by forming passive films upon the surface. This can also develop when exposed to air, also existing through chemical treatments, and exemplified through nitric acid treatment on austenitic steels. If the film is left intact, the surface will generally not undergo any form of corrosion [4, 11]. Examples of constant attack would be tarnishing of silver, green patina of copper, and the rusting of steel.

Microorganisms can either enhance the rate of corrosion or slow it down by colonising the surface of a uniform corroding material in a manner that would either form protection across the surface or cause other corrosive effects, many of which are shown in Fig. 2. Microbe adhesion to surfaces is critical for many ‘ideal’ living circumstances, which include resistance to external effects such as temperature, pH, and even biocidal substances. Microorganisms and their metabolites and extracellular polymeric substances (EPS) produce biofilms because of this surface proliferation. Biofilms practically coat any material surface that encounters water. The homogenous nature of the material’s surface makes it a very suitable site for microbial colonisation. Uniform corrosion will usually entail through SRB, which may

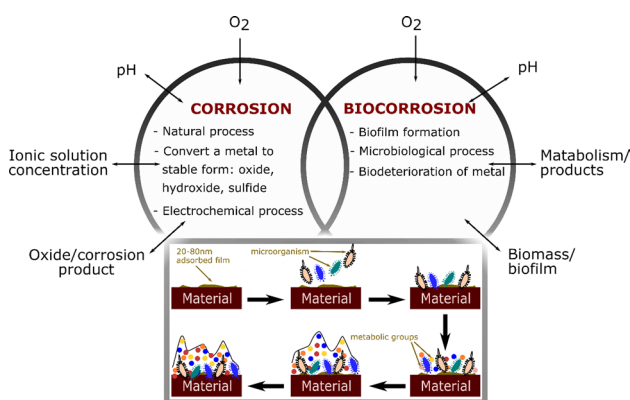
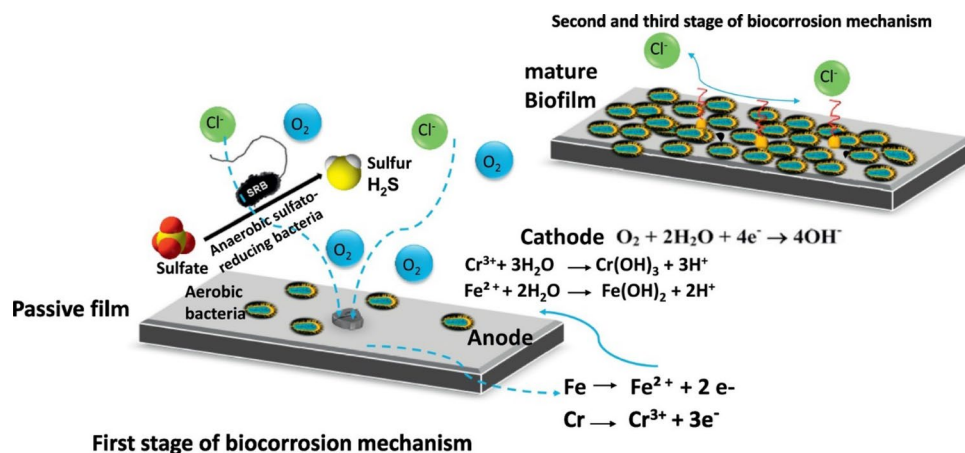


Fig. 1 Various factors influence corrosion versus biocorrosion—here, we show the formation of the microbial biofilm involved in the biocorrosion process

Fig. 2 Schematic illustration showing the involvement of various microbes such as aerobic bacteria, anaerobic sulphate-reducing bacteria in the biocorrosion mechanism of 304 L SS (obtained with permission from [20])

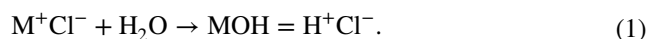


form oxides of their metabolic processes and further enhance the rates of corrosion [17–19].

Pitting is one of the most destructive forms of corrosion and is one of the hardest types of corrosion to detect because of corrosion-based products often filling the holes [21, 22]. The pitting process is unpredictable, as the process is autocatalytic and often requires a varied amount of time to process. Once the pitting process begins to evolve, the length of time a material ‘holds up’ could be a matter of days (depending on the overall environment), so the failure of the material could occur suddenly [23, 24]. Pitting corrosion is different in the initiation stages, whereas crevice corrosion is initiated by a differential change in concentration of oxygen or ions surrounding the electrolyte [25–27], where the material alone initiates pitting. Microorganisms, in theory, could, therefore, enhance pitting corrosion in terms of their excretion products, which causes further and subsequent degradation to the material [28–30]. Further pits ensue across the surface of the material, where the natural pitting process will continue to propagate.

Crevice corrosion is another form of localised attack on a material, mainly occurring in areas of narrow spaces on metal–metal and non-metal–metal interfaces. Sometimes, the material is shielded in certain areas that are exposed to corrosives, which protects against this crevice action [31, 32]. The attack is the result of high concentrations of cells formed between the electrolyte and the crevice. Usually, the crevice will become oxygen starved, and the surrounding electrolyte will gain oxygen, causing this crevice system to exist. Therefore, the material within this crevice system is acting as the anode, and the exterior will act as the cathode, completing the redox system. An example of this would be SS that is corroding in a neutral aerated sodium chloride system. The anodic metal dissolution reaction within the crevice, $M \rightarrow M^{n+} + ne^-$, is balanced by the cathodic reaction on the adjacent surface, $O_2 + 2H_2O + 4e^- \rightarrow 4OH^-$. This increase in M^+ ions within the material crevice results

in an influx of chloride ions, resulting in a net neutralisation reaction. An acidic reaction is then established, whereby releasing a free acid through the hydrolysis of the metal chloride, in Eq. 1:

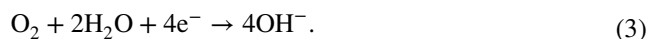


The free acid produced by the hydrolysis reaction keeps the pH below 2, while the pH outside the crevice remains neutral [33]. This microenvironment and pH state mean that the electrolyte present within the crevice has a high concentration of hydrochloric acid also containing metal chloride ions, which are dissolved at concentrations near-total saturation.

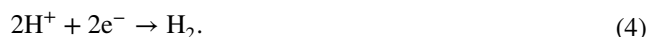
Briefly, in both the aerated and deoxygenated solutions, the anodic reaction is always metal dissolution as shown in Eq. 2:



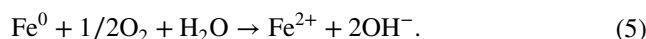
However, the reverse cathodic reaction depends on the solution conditions. For aerated solutions at neutral or alkaline pH, the main cathodic reaction is the reduction of oxygen as given in Eq. 3:



In addition, with all types of de-aerated solutions, as well as in aerated and acidic solutions, proton reduction occurs as seen in Eq. 4:



When ferrous materials begin rusting, we know this to be the most common type of corrosion. In the presence of oxygen and water, the new chemical reaction for iron rusting can be expressed as in Eq. 5:



Microorganisms present in a crevice corrosion system can cause more severe effects as a differential oxygen system is established [34–36]. Having two different oxygen concentrations at two locations will cause a difference in electrical potential and consequently produce corrosion currents. Where a crevice exists, this gives the possibility of setting up these parameters, meaning that respiring microbial colonies become anodic, causing the surrounding areas to become cathodic. Some metals develop a natural surface film or oxide layer that is a natural barrier for the stresses that erosion–corrosion brings to them. The ability of these films to protect the metal depends significantly on the speed it takes for them to be removed [37–39]. Therefore, a more complex and increased dense layer yields better protection than removed by mechanical action through ‘wear and tear’ as shown in Fig. 3. A film that is too brittle or cracks is not thoroughly protected. It is the film or surface coating that SS relies on for their inherent corrosion resistance.

Consequently, the materials will be vulnerable to corrosion in some way. The erosion–corrosion of a stainless steel type 316 (18Cr–12Ni) from a pectin extraction plant vessel was increased as temperature increased [40]. This vulnerability brought about a modification in the hydrodynamics, causing steam to increase the rate of corrosion attack [41]. The erosion–corrosion property of the steam has a stripping effect that lowers a dissolved oxidant gas, thus, causing an increased level of corrosion in the column of the distillation unit [42].

Erosion corrosion of a material is linked to the aggravation of the corrosion process [44, 45]. For instance, if microorganisms are present in a system whereby

erosion–corrosion is prevalent, the microbes can attach to the eroded surfaces of the material, thrive, and excrete by-products that could enhance the overall corrosion process. In a comprehensive review by Cheung and Gu [43], the authors summarise the mechanisms of hexavalent chromium detoxification by microbes (Fig. 4). This process, in turn, has some benefit to the erosion–corrosion system; if microorganisms are allowed to build up, thin films will be beneficial in coating the points where erosion occurs, as they are small and localised [36]. This localisation of erosion, in turn, protects the material from the corrosive electrolyte, thus, reducing the problem temporarily to the survival or timescale of the biofilm [46, 47].

Some methods of prevention that could be employed to combat this erosion problem are choosing materials less susceptible to erosion, better the design of the system to which the materials will be employed, limiting enrichments that the materials are exposed to, and employing surface protective materials coatings [48–50].

Dealloying is known as selective leaching, parting corrosion, or selective dissolution and is an essential electrochemical process associated with alloys formed by components with different noble characters (with varied standard equilibrium potential) [51, 52]. Nobler component phases, formed during the dealloying process, play essential roles in stress corrosion of cracking metallic surfaces, but selective dissolution can be utilised via suitable technologies [53, 54].

In the dealloying process, one of two mechanisms can occur: alloy dissolution and re-plating the cathodic element or selective dissolution of an anodic alloy component. Both cases leave a spongy and porous metal, and all aspects of shape, rigidity, strength, and ductility are sacrificed. As with other types of corrosion discussed, the prime cause of the selective leaching effect is the galvanic reaction between the elements. Examples of alloy combinations and elemental leaching are described in Table 1.

3 Analytical Methods in MIC Characterisation

Many methods have been used over the last few decades to measure and determine corrosion rates. Ever since the first report of corrosion in 1910 until the present, techniques have developed and evolved. Some of these methods have not been explicitly designed for biocorrosion analysis and have merely been adapted. In this section, we report the state-of-the-art characterisation techniques for MIC and the processes of corrosion.

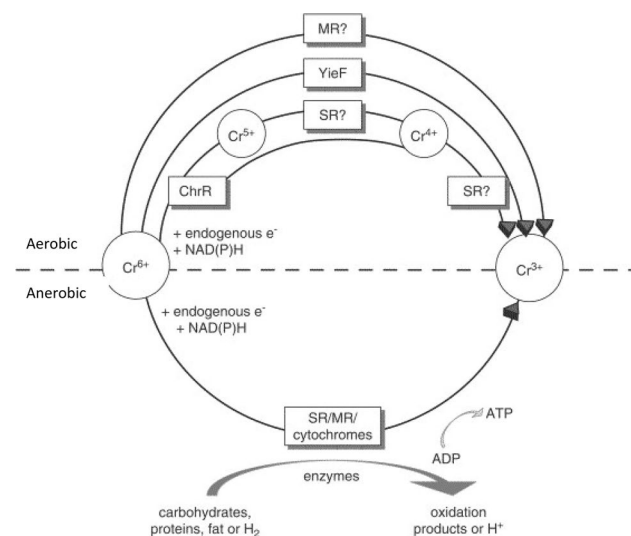


Fig. 3 Proposed biochemical pathway showing the reduction of Cr^{6+} enzymatically under aerobic and anaerobic conditions mechanisms of enzymatic Cr^{6+} reduction under aerobic (upper) and anaerobic (lower) conditions (obtained with the permission from [43])

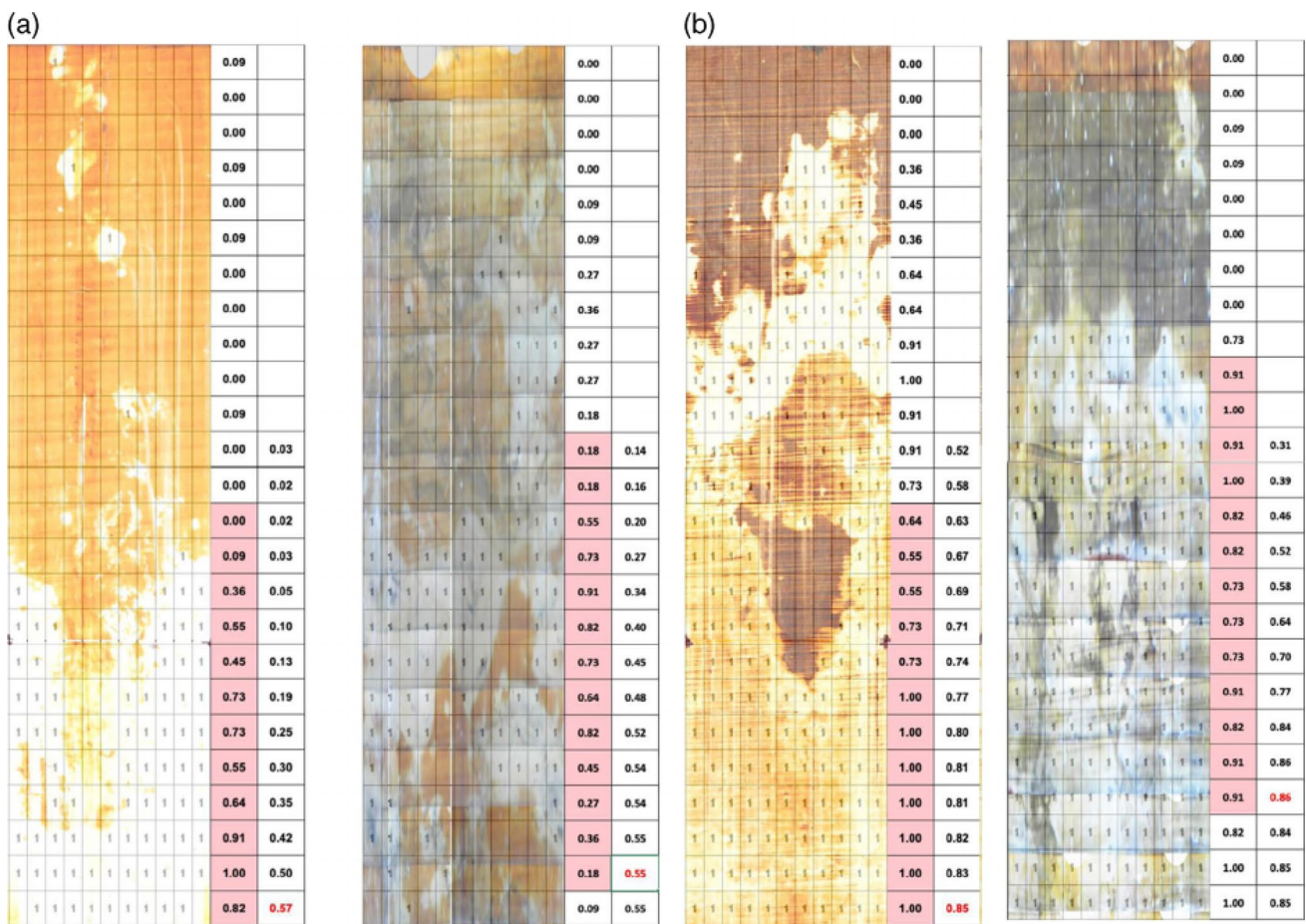


Fig. 4 Use of borescope images to show **a** (left) iron oxide and (right) clear. **b** Sample borescope images of manganese-oxide borescope images. A value of 1 was assigned if manganese oxide was removed or replaced with iron. The yellow colour is the abiotic iron-oxide

replacement of the manganese oxide (Color figure online). Reproduced with permission from CCC Rightslink, Soil Society of America

Table 1 Alloy combinations and elemental leaching

Alloy	Environment	Element and dealloying term	References
Brass	Many waters, incredibly stagnant, or low aeration	Zinc (dezincification)	[55]
Grey iron	Soils, most waters, engine blocks, and low tensile strength required housing	Iron (graphite corrosion)	[56]
Aluminium bronzes	Hydrofluoric acid, acids containing chloride ions, non-sparking environments	Aluminium (dealuminification)	[57]
Copper nickels	High heat flux and low water velocity (e.g. condenser tubes—refineries). Offers exceptional resilience to corrosion of seawater	Nickel (denickelification)	[58]
Gold alloys with silver or copper	Sulphide solutions, human saliva	Copper, silver	[59]
Medium and high carbon steels	Oxidising atmospheres, hydrogen at high temperatures	Carbon (decarburisation)	[60]
Iron-chromium alloys	High-temperature oxidising atmospheres	Chromium, protective film	[61]
Nickel–molybdenum alloys	Oxygen at high temperatures	Molybdenum	[61]

3.1 Borescope

A borescope is an optical-based device, which enables online visual inspection of the internal surfaces of pressurised vessels and reactors. Chiavari and co-workers implemented a borescope to measure visible corrosion in historical tubes of a pipe organ. This measurement was achieved using a 37.5 cm borescope with a digital camera attachment [62]. Borescopes currently available do not support high-resolution inspection or automation. A recent study proposed a hyperspectral imaging (HSI) probe for corrosion monitoring that enables high-resolution scanning and automation [63]. Compared to RGB images, the proposed HSI modality captures reflectance at multiple wavelengths from multiple spatial points on the sample and provides an enormous amount of spectral detail. A key research area that has been developed as a strategy for automatically detecting corrosion on aeroplane structures using images taken by a borescope and also using deep neural networks (DNNs) has been reported by [64]. The authors demonstrate that a robust model could be developed using a dataset that included D-Sight Airplanes Inspection System (DAIS) photos from various lap joints on Boeing and Airbus aircraft. With a precision of more than 93%, this study proved that the use of DNNs can help reduce uncertainty caused by operator tiredness or insufficient training. This technology enables rapid, non-contact corrosion inspection, and the flexible fibre probe, which functions similarly to a borescope, can be utilised to inspect difficult-to-access locations. Although primitive in the determination of corrosion or indeed rates of MIC on a material, the borescope has been taken to advanced levels. For example, Scott et al. [65] used the borescope to create images of corrosion of metals in soils which bacteria were facilitating. Indicator of reduction in soils (IRIS) is an important technology for identifying hydric soils. However, the method does not allow real-time analyses. The authors-built sample images that were scanned and then given a value of 1 if iron oxide was removed (Fig. 4). The method can be paired with Wi-Fi and, thus, continuous monitoring applied to the system. The authors set out to measure the rates of microbial influence and identify the bacteria responsible for the removal of the metal oxides—however, this proved difficult.

3.2 Thermal Imaging and FTIR

Thermographic imaging is a valuable tool for detecting less visible forms of corrosion. It has the advantage of scanning vast areas with high throughput to provide a more comprehensive view of simple structures. The method is fast and non-intrusive but does not offer a cost-effective way to quantify low levels of corrosion. At low levels, the images lose clarity, and layered structures provide a problem. Mabrouki and colleagues investigated vibro-thermographic methods

for detecting fatigue cracks in steel [66]. This technology is close to that used in electromagnetic shakers or ultrasonic burst actuators. The study focused on the efficient use of thermal imaging technology to predict fatigue cracks. Another work employed a dual-band infrared tomography system to seek out aircraft imperfections and hidden corrosion [67]. Also, the infrared thermography was used to investigate the fatigue performance of structural steel under the laboratory and actual corrosive environments [68]. This system offers more excellent resolution in imaging and, therefore, better detection of surface corrosion.

An excellent use of thermography was demonstrated for concrete by Vishwakarma et al., where the authors used lock-in thermography (LT) phase angles and amplitude images were compared between unexposed and exposed concrete specimens to characterise deterioration under biofilms. Fly ash-modified concrete showed least pH reduction and least density of total heterotrophic bacteria, SRB and SOB in the biofilms. In order to carry out the method, the authors used that a CEDIP Silver 420 camera was used for the study with thermal resolution of 25 mK. Two halogen lamps of 1000 W power each were used as optical light source. A function generator and an amplifier were used for generating sinusoidal stimulation. The samples were kept at a distance of 40 cm from the camera [69].

Attenuated total reflectance Fourier transform infrared spectroscopy (ATR–FTIR) has been used to quantify rates of dissolution of thin metals. Changes to the atomic layers of thin metal can be measured using ATR–FTIR by non-destructive means and in real time. For example, Bremer and Geesey used ATR–FTIR to monitor bacterial interactions on copper in both static and flowing conditions [70]. Additionally, the use of FTIR to study material degradation in the presence of microbes was used by Nasrazadani et al., where FTIR was used to identify concrete degradation due to biogenic sulfuric acid attack. Concrete samples were exposed to electrolytes containing bio-species in laboratory-simulating field conditions and FTIR spectra of the reacted concrete were analysed for concrete phase formation. *Streptomyces* sp. was subsequently isolated and identified using S16 RNA sequencing which was then used as the biogenic medium to simulate MIC in the concrete samples which was then analysed using FTIR [71].

3.3 Atomic Force Microscopy (AFM)

AFM was first used in 1986 and is considered a foremost tool in nano-imaging and manipulation [72]. It has become a ubiquitous method in terms of the ability to characterise a surface at nanoscale, showing topographies that covers the show. It is an exact technique that provides topological and compositional information about a wide range of materials. These can include living cells, ceramics, or high-strength

steel. This is useful in understanding how microorganisms interact with a substrate, where they attach, and how they further colonise. Although AFM is not commonly used in corrosion studies, it has been successfully used for in situ electrochemical studies. Other authors performed an in situ electrochemical atomic force microscope to investigate pitting corrosion on Cu films [73].

AFM has two main modes of operation, contact and non-contact. Contact mode is the basis for all AFM techniques in which the probe tip is in physical contact with the sample surface of the material. While the tip scans along the surface, the sample topography induces a vertical deflection of the cantilever, producing high-resolution surface topographical images [74]. Corrosion measurements were performed using AFM in both modes (contact and non-contact) to measure levels of corrosion on stainless steel SUS304 deposited with sulfuric acid [75]. An excellent example of work showing high-resolution AFM of MIC was demonstrated by Xu et al. [76]. This work shows high-resolution topological imaging of bacteria that are attached to steel surfaces. The AFM work showed not only single-cell SRB with EPS production but also SRB clusters [76]. AFM can also be used to assess various corrosion inhibitors such as non-ionic surfactants. Mu and Li investigated the inhibition action of Tween-20 with sulfuric acid on SS [77]. Olivares-Xometl et al. performed similar work where imidazolines and amide precursors derived from oleic acid were evaluated as a corrosion inhibitor on steel, which can be seen from the AFM images that the corrosion inhibitors formed a film across the surface of the steel [78]. More recently, Yuan and co-workers have used AFM to evaluate the biofilm colonisation dynamics of *Pseudomonas* NCIMB 2021 and *Desulfovibrio desulfuricans* ATCC 27774 on 304 stainless sheets of steel [79]. This was achieved by measuring the forces and interactions of the tip of the biofilm and the stainless-steel coupon surface.

Electrochemical atomic force microscopy (EC-AFM), a subfield of scanning probe microscopy (SPM), is capable of high-resolution imaging of substrate topography (Fig. 5) [80]. It has been expanded to a diverse variety of research areas by continuous improvement since its inception. The presence of an electrolytic cell and a potentiostat enables real-time observation of the sample surface's topographical changes. EC-AFM is used in situ corrosion research because electrically conductive samples are not required. EC-AFM operates similarly to AFM, with the instrument can be controlled in either constant height or constant force mode. The imaging method is commonly classified into different operating modes based on the interaction force between the tip and the sample, including touch mode, non-contact mode, intermittent tapping (tapping mode), torsional resonance mode, and peak force-tapping mode. The first mode is touch,

in which the probe's tip is often in contact with the sample's surface, and the force between the tip and the sample is repulsive. Due to the softness of the silicon nitride cantilever and its high resonance frequency, which prevents vibration instability, a silicon nitride probe is often used in touch mode. Although the contact mode offers superior resolution and scan speed, it can cause damage to the sample's surface.

In conclusion, AFM is a very versatile technique with an array of use in biocorrosion studies. The method has some drawback; due to its sensitivity, it is susceptible to environmental interferences, i.e. vibration. The technique is also very time consuming due to its accuracy and results often must be treated for errors that exist.

3.4 Scanning Electron Microscopy (SEM)

SEM is a technique that is paramount and routine in determining biofouling and biocorrosion on a substratum. SEM has been used in many scientific papers and has become a susceptible and highly effective technique in identification, analysis, and characterisation [81–93]. For examples, field emission scanning electron microscopy (FESEM) and AFM were used to characterise the dimensional morphology of the SS after pitting [94]. It was shown that the bacterial adhesion increased with the pH and temperature, which significantly increased the surface roughness of the SS. SEM and AFM analyses showed cracks and dislocations on the surface of stainless steel underneath the attached bacteria, which suggested a direct role of biofilm in corrosion induction.

The technique is often coupled with energy dispersive spectroscopy (EDS) and has been extensively used to demonstrate bacteria in corroded areas with the determination of surface chemistries from MIC [95–97]. The elemental chemistry of the base metal can also be determined using the EDS tandem with SEM. The preparation of biological material requires manipulation and fixation with some samples requiring dehydration or critical point drying because the SEM operates under high vacuum [98, 99]. Also, non-conducting samples, inclusive of biofilms, must be coated with a thin film of metal before the specimen can be analysed, usually known as 'sputter-coating'. If the sample was uncoated, a build-up of local electrons would occur, this is known as sample 'charging', and the imaging is regarded as unusable owing to localised charge effects superimposed over the detail of the image. EDS can be used to determine the elemental composition of a surface; this can only be achieved before sputter coating. EDS samples are collected from a specific area, removed from the sample chamber, sputter coated, and then returned to the sample chamber. This can cause problems as more than often, the sample will not be in the same place, so reproducibility in the position is often difficult. Sample preparation for SEM, inclusive of

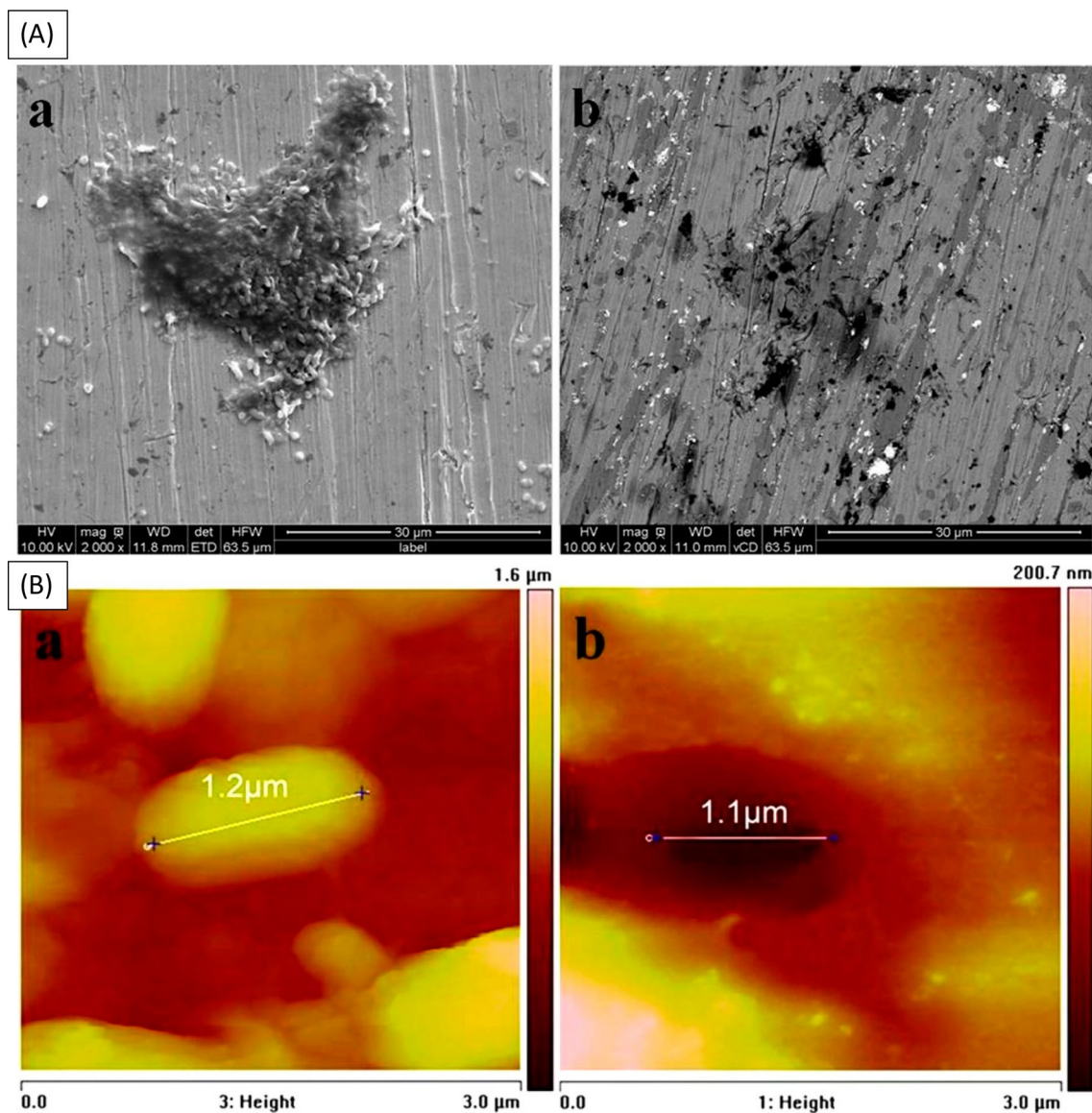


Fig. 5 **A** SEM micrographs showing the surfaces of steel substrates (a) prior to and (b) following biofilm and corrosion by-product removal. For 90-day incubation, these substrates were initially incubated in the synthetic saltwater containing *Bacillus* sp. Following that, the surface was cleaned of biofilm and corrosion by-products.

B Atomic force microscopic images showing the surface topography of the steel plates after submerging in artificial salt water for 90 days (a) before and (b) after biofilm removal, demonstrating the apparent pitting of the steel samples following biofilm removal (permission obtained from <https://www.mdpi.com/2079-6412/10/10/983/htm>)

solvent removal, and drying can decrease the areal surface by the biofilm, as Little et al. [100].

Some shortcomings of SEM and EDS come in the form of peak overlap in the data and spectral data output. For example, spectral peaks for sulphur overlap with those of spectral peaks for molybdenum, thus, highlighting that for materials and corrosion aligned with MIC can be problematic. In addition, the characteristic peak for manganese coincides with the secondary peak for chromium highlighting that that data need to be carefully analysed. In order to reduce these

limitations, wavelength dispersive spectroscopy can be used to resolve overlapping EDS peaks.

Another area of SEM that is becoming more widely used is ‘environmental scanning electron microscopy’ (ESEM). The method is fast and accurate imagery can be obtained based on less vacuum and more appropriate imaging without the need for exhaustive sample preparation. The technique uses unique secondary electron detectors to form high-resolution images at pressures ranging from 0.1 to 20 Torr. Charging is dissipated into a gaseous form in the chamber

at these pressures, enabling direct observations of uncoated or non-conductive samples [101].

Gregerová and co-workers used SEM as a technique for the identification of corrosion in concrete [102]. They state that it is an effective tool in analysing deteriorating material properties, mentioning that concrete is being attacked by sulphate and carbonation. Although this is true, consideration should have been given to microorganisms attributing to the further corrosive action surmounted by biological means instead of pure chemical processes.

In short, SEM offers detailed structural topographical imagery. It can visualise flaws in materials but also highlight any microorganism attachment upon a substrate, especially in biocorrosion. Sample preparation is relatively simple and does not require a lengthy preparatory approach. The method has some disadvantages such as sample charging, the ability of reproducibility is limited and time consuming.

3.5 X-Ray Photoelectron Spectroscopy (XPS)

XPS has been routinely used for quantitative surface composition analysis. Relative elemental concentrations are determined by comparing intensities of the characteristic signals [103]. XPS is excellent at quantitatively analysing outermost passive layers on a surface and has evolved as a predominant technique in biofilm analysis. Gregerová and co-workers used XPS to determine concrete composition from the Charles Bridge in Prague, Czech Republic [102]. This could be useful in determining an initial and final sample point and seeing the changes in composition and applied to further biocorrosion samples or environments. Yang and co-workers have analysed the surface morphology of magnesium alloys, and XRD was applied to monitor the biocorrosive characteristics for medical application [104]. X-ray photoelectron spectroscopy was used to study the interactions of an exopolymer-producing bacteria, *Burkholderia* sp., with polished AISI 304 SS substrates (XPS) [105]. Another excellent example of how XPS is an excellent technique in determining what compounds and effects are causing biocorrosion.

XPS, unlike SEM and EDX, produces far lower kinetic energies for Auger electrons and X-ray-excited photoelectrons than those of fluorescence X-rays generated by the electron beam in a SEM. This lower energy produces meaningful information when they are not attenuated by surface layers; namely the photoelectrons and Auger electrons from a few monolayers of the top of the surface are characteristic elements and molecules in these monolayers [106].

Juzeliunas et al., measured the rate of corrosion on zinc and aluminium in a two-year long study using fungi. *Aspergillus niger*, a filamentous ascomycete fungus, was isolated from the metal samples exposed to marine, rural, and urban

sites in Lithuania, Europe. Al and Zn samples were subjected to the influence of *A. niger* under laboratory conditions in humid atmosphere for two years. The use of electrochemical impedance spectroscopy (EIS) ascertained microbially influenced corrosion acceleration (MICA) of Zn and MIC of Al. The surface analysis was carried out by XPS where the surface sputtering by ionised argon showed significant content of organic carbon within the layer of the material. The highest content of organic carbon was found on the top of the corrosion product layer (ca. 40 at.%), which comes from the dehydrated microorganisms and their metabolites. The noticeable concentrations of organic carbon were found to be in deeper levels (8–10 at.%) which have to be considered as the result of the organic acid penetration into the corrosion product layer, the authors provided this evidence as they did not find the carbon in the XRD data, highlighting that the multi-instrument analysis principles are imperative to corrosion studies [107].

3.6 Optical Microscopy (OM) and Epifluorescence Microscopy (EM)

OM is likely to be the oldest technique in visually characterising the level of corrosion that a material has suffered in more depth. Few researchers utilised this method to analyse bio-based films and immediately use SEM to characterise a surface. OM can evaluate biological-based material microstructures and has been done by Veiga-Santos et al. [108]. The technique offers excellent visual imaging of the sample, including colouring and hue depth, with the only limitation is that it cannot directly measure forces that biological samples exert on surfaces, such as bacterial populations upon a substrate. This limitation can be overcome if combined with other techniques, for example, with AFM, which can measure forces of attachment by using the cantilever as a force measurement [109]. Another form of microscopy closely linked to OM is EM, and this will document numbers of bacteria present upon a surface and enumeration. EM has been used to evaluate the distribution of cells on a surface but requires a certain level of sample preparation. The sample needs to be fixed and stained (Fig. 6). It is often hard to distinguish individual cells within densely populated regions on the sample and can often be impossible to image with corrosion-based samples as the stain and products are impenetrable.

Confocal scanning laser microscopy is emerging as a combinational approach to distinguish material and MIC. For example, in a study by Arun et al., the MIC of UNS S32750 super-duplex stainless-steel joints fabricated was investigated using different welding methods. The authors introduced the sample into a medium inoculated with *Micrococcus equiperdicus* isolated from a marine environment. The study found that when CLSM and AFM

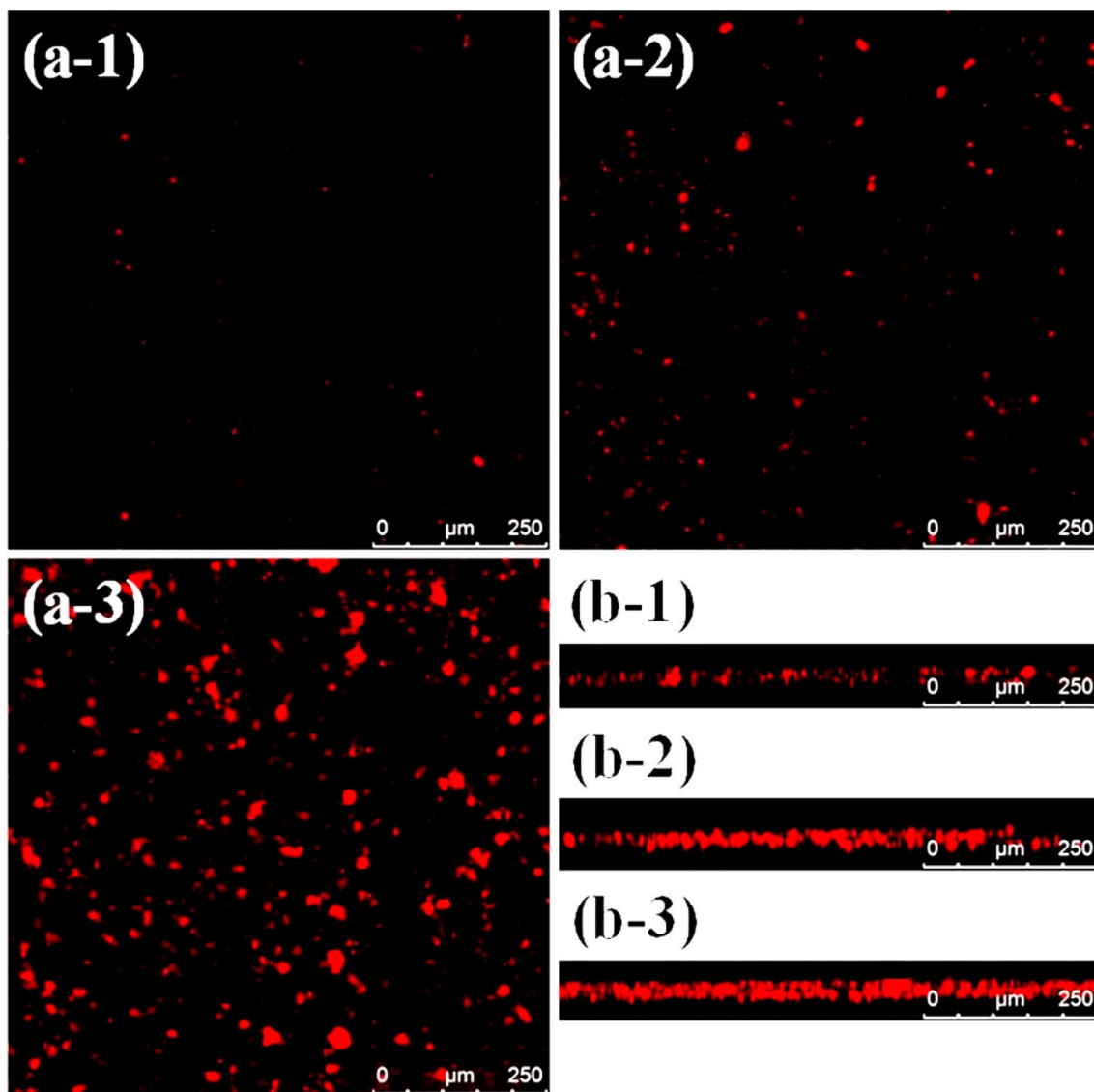


Fig. 6 Fluorescent micrographs showing the biofilm formation of *Bacillus* sp. on the steel surfaces which were incubated after **a-1** 1 day, **a-2** 1 week, and **a-3** 1 month and side view images **b-1** 1 day,

b-2 1 week, and **b-3** 1 month. Cross-section micrographs showing the thickness of formed biofilms on steel substrates (adapted with the permission from <https://www.mdpi.com/2079-6412/10/10/983/htm>)

could readily characterise the topography and formation of pits in the corroded samples. The authors successfully used CLSM for surface morphologies and the width of the pits of the SS materials which were then turned into 2D and 3D interpretations created when in combination with AFM [52].

Interestingly, a material known to be relatively solid and robust was found to corrode when subjected to *Pseudomonas aeruginosa*. For example, Khan et al., found that MIC of pure titanium when studied using CLSM demonstrated pitting corrosion. The pitting corrosion was investigated with the help of CLSM, and the largest pit

depth found on Ti surface immersed in *P. aeruginosa* was 1.2 μm . The study highlighted that Ti was not immune to MIC caused by *P. aeruginosa* [110]. CLSM is fast becoming a method of analysis for pitting corrosion with many authors already using the microscopic method [111].

3.7 X-Ray Diffraction (XRD)

XRD is widely used in works concerning corrosion. It works on the principle where X-rays are scanned to the surface of the sample, and a signature relay is measured, giving a signature for each element present. Reyes et al. investigated

the MIC of copper pipes at a low pH. This was to simulate the drinking water conditions in a typical rural home [112]. They took various sections of the water system's copper pipes and analysed them using XRD. The analysis told them that the biofilms were growing around malachite that had formed due to oxidation of the copper pipe. Dinu et al. monitored biomedical alloys for the growth and deposition of unwanted bacteria; hydrogen was tested as an alloying element, and analysis was performed using XRD, another use of characterisation using XRD [113]. Gebert and co-workers analysed structural states of corroding NiMnGa alloys for memory applications [114], with XRD. Christina-Cardona and co-workers utilised XRD to characterise native microorganisms that inhabited two coal types [115]. XRD was used to measure the depletion of pyrite peaks in the sample, thus, illustrating that microorganisms assisted in the breakdown of the coal samples.

Calle and co-workers performed leaching studies upon copper pipe in a household-plumbing system [116]. Microorganisms were deemed problematic in adding to the corrosion problem through biofilm attachment. XRD was used as a means of determining copper leachate. This needed to be further resolved with X-ray absorption spectroscopy, which then identified the species of copper released on the flux of the copper piping.

In a study by Khouzani et al., MIC on pipelines from a petrochemical plant was investigated. The authors utilised several techniques; however, they showed that the typical XRD patterns of corrosion products, taken from the surface of the pipe, could be successfully evaluated. The results showed that iron was present in the biofilm and on the material, showing that the biofilm was using the pipe system to facilitate corrosion. The authors showed a typical XRD pattern of corrosion products, confirming the formation of a significant amount of oxide-hydroxide (FeOOH), iron oxide, and iron taken from the surface of the pipe. The results confirmed the formation of a significant amount of sulphide. The latter is a typical corrosion product when sulphate-reducing bacteria are the controlling microorganism [117].

In addition, Khanfar and Sitepu recently reported a case study of MIC and using XRD as a source of phase analysis for deposits created in a refinery. The refinery environment was from crude cooler and reboilers which were then analysed for MIC using microbial, metallurgic, and special analyses and correlates the Rietveld quantitative phase analysis of high-resolution X-ray powder diffraction (XRD) data of scale deposits with microbe compositions. Therefore, rapid in-field microbiological assays could be carried out to assess the potential of MIC. Based on the results, it can be highlighted that the MIC investigation showed that total bacteria and SRB were detected in all sampling locations [118].

3.8 Electrochemical Methods

An electrochemical method is a recent technique introduced to detect and monitor corrosion [82, 119, 120]. Most of these methods are governed by change by electron transfer within a sample as the basis of detection. The techniques covered are linear polarisation measurements, electrochemical impedance spectroscopy (EIS), electrochemical noise (EN), and mass spectrometry (MS).

3.8.1 Linear Polarisation Measurements

A linear polarisation technique can coherently measure the rate of corrosion based upon the Stern-Geary equation in Eq. 6 [121, 122]:

$$I_{\text{corr}} = K [\Delta I / \Delta E], \quad (6)$$

where corrosion current I_{corr} is deduced from corrosion test coupons [i.e. stainless steel (SS)], ΔI is the change in current, and E is the change in potential. This is where the Tafel slope of K can be evaluated. There are limitations to this equation, with slight differences in the environment inflicting limitations in the accuracy of I_{corr} and K . Therefore, it can only be achieved in specific environments but gives excellent results.

Linear polarisation can also be harnessed, measuring the resistance, and is a common electrochemical technique called linear polarisation resistance (LPR) [123]. LPR is an excellent chemical technique for measuring continuous rates of corrosion. Here, R_s (the solution resistance) between the corroding interface (i.e., the metal) and the reference electrode, and the polarisation resistance R_p is related to the corrosion rate. LPR requires a potential scan or stepping sequence that varies the probe's potential concerning the corrosion potential E_{corr} . The technique has been used across industrial sectors to monitor corrosion rates, which was historically constrained to aqueous environments. More recently, probe technology has advanced, and high resistance and atmospheric exposures can now be monitored [124]. Habib and Bouresli developed an optical sensor for the active detection of corrosion in 304 and 316 SS. This was achieved by basing the metre on 3D holographic interferometry to measure micro-surface dissolution, i.e., mass loss. This was principally achieved through LPR [125].

3.8.2 Electrochemical Impedance Spectroscopy (EIS)

EIS has been applied to corrosion systems for over 30 years and is now a powerful tool for corrosion analysis [126, 127]. An advantage of using EIS over other laboratory techniques is the leeway of using small-amplitude signals without disturbing properties being analysed. EIS studies the system

response to the application of a periodic small-amplitude ac signal. EIS can determine the polarisation resistance (R_p), which is related to the rate of corrosion. EIS also provides a solution resistance (R_s) and mechanistic information and adds extrapolating to a steady-state condition. This is beneficial as it allows for improved corrosion rate estimations. Guo et al. compared weathering resistance steels and weathering steels that are contained in performance bridge steel [128]. EIS results showed that rust layers of the resistant steels were more significant than the weathering steels.

Wenger and co-workers investigated open-pit morphologies upon an AISI 430 steel electrode using EIS [129]. Pits were initiated by using a sulfuric acid solution containing sodium chloride, where it could be noticed that pit morphologies could be related to fluctuations in impedance data. Gabrielli and co-workers investigated pit propagation using EIS in iron [130]. The pit morphologies were different from Wenger et al., as they were initiated using a scanning electrochemical microscope method (SECM). This method brings about a means of generating localised and controlled amounts of chloride ions.

3.8.3 Electrochemical Noise

EN involves measuring the electrochemical transient noise produced by the corrosion process [131, 132]. This is accomplished by measuring the potential noise of the potential difference between two identical electrodes or by tracking current differences between two similar electrodes using a zero resistance ammeter [133]. EN was initially designed to monitor corrosion such as pitting and crevice. EN recognises conditions versus stability, i.e., low noise to random events of material's lifetime. Mansfield and co-workers developed EN to monitor both the initiation and propagation of stress corrosion cracks [134]. They developed electrochemical impedance and noise measurements taken bi-weekly through remote control modem access at Key West, Florida, over 9 months of three polymers coated to SS. Analyses were performed in the time and frequency domains. Conclusions were drawn that through the electrochemical analysis, a polyurethane topcoat fared better than the latex coating [134]. All electrochemical methods are averaging techniques that work best when the chemical and electrochemical conditions on the metal surface are uniform and at steady state, this is important when understanding MIC on the surface of a material.

3.9 Spectroscopic Techniques

The continuous proliferation of new bacterial species presents microbiologists with an ongoing typing challenge. Although molecular biology techniques are essential for bacterial typing, they are often laborious, time consuming, and

inevitably fail when dealing with very closely related organisms. When paired with chemometric approaches, spectroscopic techniques can be a feasible alternative to molecular methods in some instances, providing advantages in terms of analysis time and expense. For examples, a combination of ATR-FTIR and chemometrics revealed significant spectral differences below 1400 cm^{-1} , which is frequently associated with phosphate and carbohydrates molecules [135]. PCA and HCA revealed three distinct clusters, each containing isolates from a single genus. Janbu et al. have used FTIRS and FTIR micro-spectroscopy to distinguish five *Listeria* species [136]. The performance rates of discrimination obtained were approximately 93 and 100%, respectively. The stepwise canonical discriminant analysis (SCDA) and partial least-squares regression discriminant analysis were used to obtain these findings.

As early as 1998, there were reports of FTIR being used to measure MIC by Hans-Curt Fleming and his team [137]. FTIR spectroscopy is suitable for the identification of micro-organisms and presents a new addition to taxonomic and genetic characterisation methods. The FTIR analysis of bacterial isolates provides fingerprint spectra, allowing for more rapid characterisation of microbial strains and in complex matrices. When combined with the principles of attenuated total reflection (ATR), the FTIR-ATR technique can be used for the observation of biofilms forming directly on the interface of an ATR crystals such as germanium. Spectra can be acquired non-destructively, in situ and in real time. For example, Chapman et al. have recently been using FTIR and NIR systems to study microbial proliferation and reactions to antibiotics [138–141].

3.10 Mass Spectrometry (MS; Biochemical)

While many of the previous methods are used for imaging, MS can characterise complex molecular systems. More particular to corrosion analysis, secondary ion mass spectrometry (SIMS) has been used to determine the metal ion distribution in SS. Salaita (1995) reported using SIMS using a liquid metal ion source (LMIS) to achieve high-resolution chemical maps of the surface [142]. SIMS can yield images with high sensitivity and lateral resolutions of 100 nm or improved. The technique is primarily used for metal and inorganic materials. Severe limitations exist with SIMS, the first being that it is destructive to any organic surface layer, and second, extensive ionisation patterns make it challenging to analyse large molecules.

Matrix-assisted laser desorption/ionisation-mass spectrometry (MALDI-MS) was used to detect the polysaccharides produced in a complex biofilm composed of a mixed consortium of marine microbes. For example, corrosion of aluminium exposed to seawater caused by a marine fungus was observed, and the fungus was identified using

MALDI-MS analysis of EPS [143]. Rapid, responsive, and direct MALDI-MS analysis of biofilms will significantly accelerate and expand our understanding of biofilms due to its outstanding advantages, such as simplicity, high sensitivity, high selectivity, and high speed. MALDI-TOF introduces a new, rapid, responsive, and selective platform for studying biofilms in natural water that eliminates the need for time-consuming culture steps or complex sample pre-treatment procedures.

In a paper by Beale et al., a novel application using fluorescence spectroscopy and GC-MS to analyse water samples exposed to copper piping which had undergone some degree of MC was carried out. Using 3D fluorescence spectroscopy, the author observed a 'protein-like' fluorophore associated with the presence of bacteria, which was then cross-referenced with a series of derivatized fatty acid metabolites determined using GC-MS. This methodology was shown to be effective and simple as a screening tool to establish the presence of any microbial processes in waters and then correlate specific metabolite profiles with different microbes which again showcases an effective combinatory approach for MIC analyses [144].

More recently, the spatial distribution of microbial metabolites has become important, as the identification of metabolites for establishing the significance of these metabolites to MIC poses as important biochemical information to understand the processes of MIC and, thus, to provide valuable information for more precise mitigation techniques or methods. As MIC is a localised phenomenon, it is likely that the metabolites present at the biofilm-metal interface are more relevant to the processes linked to MIC. While most MS methods cannot be used for deriving information on the spatial localisation of metabolites, new and emerging MS techniques such as imaging mass spectrometry (IMS) [145] and laser ablation and solvent capture by aspiration mass spectrometry (LASCA MS) [146] can be used for in situ analysis to determine the spatial organisation of metabolites in a more complex microbial biofilm. For example, using LASCA, a recent study by Brauer et al. [146] identified that metabolites that are corresponding to anodic activity appeared in the central carbon steel samples, while the metabolites corresponding to cathodic activity occurred at the outer edges of the steel samples. This rich information based on the spatial distribution of metabolites allows for the understanding of heterogeneity of biofilms on the samples and the underlying processes of MIC, but also their impact on the intrinsic mechanisms for MIC [147].

3.11 Significance of Analytical Tools for MIC Analysis

Suitable application of analytical techniques for both the detection and monitoring of MIC is critical to understand the

mechanisms of microbial interactions with a given material and for selecting the correct inhibition, mitigatory, or control measures. This review provides the application of analytical techniques available for MIC measurement using ranges of methods such as electrochemical and surface analytical techniques. Conventional electrochemical techniques, such as corrosion potential (E_{corr}), redox potential, EIS, and micro-electrode techniques, are important for fundamental material and MIC studies. The emergence of an electrochemical quartz crystal microbalance has proved to be an important feature for the study of MIC. Microscopic techniques (SEM, ESEM, AFM, CLSM, confocal Raman microscopy) and spectroscopic analytical methods (FTIR, FTIR-ATR, NIR, and XPS) are also very important for the analysis of MIC and should be used in combination with methods. The heterogeneous characteristics of microbial consortia and use of special techniques to study their probable effects on the metal substrata are often difficult even without the issues of corrosion and material characterisation. The aim of this review is to motivate researchers to use a combination of new analytical techniques to perform practical measurements to generate meaningful data to calculate the impact of MIC and biofilms on materials. With this in mind, research will be able to progress in making more precision changes to materials to prevent MIC—for example, understanding the metabolite and often the biofilm features when interacting with a material will generate new approaches to mitigate the MIC issue, thus, producing new materials capable of resisting damage from microbes.

4 Conclusion and Future Perspectives

The long-term preservation of any material requires a holistic method for mitigation. Understanding the bio- and chemical environments that the material is immersed in will be a firm step in preventing and applying the correct counter-measures of fouling and biocorrosion. Without the aid of detection and monitoring, materials that are in contact with microorganisms will undergo rates of corrosion faster than ones that do. We have tried to capture the most important of these new trends in research and analytical methods of analysis.

Recent developments in the use of handheld systems will make it possible for online, site, and in-field measurements of MIC on materials. More attractive techniques using FTIR and NIR which are non-destructive will also play a key role in this area.

Electrochemical methods are still the gold-standard analytical method to measure the surface activity of kinetic and corrosion processes. The issue with electrochemical measurement is that the electrode surface tends to change because of the continuous electrode surface changes owing

to microbial adhesion and biofilm formation (biofouling). Noise analysis is the most typical method for the evaluation of MIC; however, its main disadvantage is the need for complex mathematical models to obtain real current and voltage values. Therefore, we recommend using tandem electrochemical techniques in order to see the corrosive interaction and deterioration of the material when measuring the MIC.

Biofilms formed in different environments which are measured either in situ, in the field, or in the laboratory on materials have been extensively investigated, and therefore, many techniques are already available for this reason. The methods of analysis provide qualitative measurements, while surface chemical techniques provide the quantitative material and composition changes caused by biofilm and MIC processes.

Fluorescence microscopy has opened the ability to visualise microbial cells on material surfaces. Once the appropriate dyes to stain the microbes are used, not only are all the microbes visible, but we also obtain information about the life cycle of the cell (e.g. live/dead). Supported by SEM, SEM can provide a quasi-3D image of single cells or colonies of cells as well as the EPS of the biofilm (although due to the preparatory process of SEM, this is typically dehydrated).

EDX can provide data on the change of composition caused by the presence of MIC. We have detailed many examples of this method for MIC determination, while the use of spectroscopic methods (FTIR and XPS) can explain why and how these methods support the understanding of MIC.

This review details many analytical techniques and explains the importance and relevance of parallel and combinatory analytical techniques to obtain the information about MIC.

Funding Open Access funding enabled and organized by CAUL and its Member Institutions. This research is part of the projects undertaken on the Infrared Microspectroscopy (IRM) beamline at the Australian Synchrotron, part of ANSTO. There were no research grants for this work from any funding agencies.

Declarations

Conflict of interest The authors declare that there are no competing interests.

Open Access This article is licensed under a Creative Commons Attribution 4.0 International License, which permits use, sharing, adaptation, distribution and reproduction in any medium or format, as long as you give appropriate credit to the original author(s) and the source, provide a link to the Creative Commons licence, and indicate if changes were made. The images or other third party material in this article are included in the article's Creative Commons licence, unless indicated otherwise in a credit line to the material. If material is not included in the article's Creative Commons licence and your intended use is not

permitted by statutory regulation or exceeds the permitted use, you will need to obtain permission directly from the copyright holder. To view a copy of this licence, visit <http://creativecommons.org/licenses/by/4.0/>.

References

1. Little BJ et al (2020) Microbially influenced corrosion—any progress? *Corros Sci* 170:108641
2. Singh AK (2020) Mitigation of microbial induced corrosion. In: Singh AK (ed) *Microbially induced corrosion and its mitigation*. Springer, Singapore, pp 107–129
3. Karatan E, Watnick P (2009) Signals, regulatory networks, and materials that build and break bacterial biofilms. *Microbiol Mol Biol Rev* 73(2):310
4. Coetser SE, Cloete TE (2005) Biofouling and biocorrosion in industrial water systems. *Crit Rev Microbiol* 31(4):213–232
5. Coghlan A (2004) Michelangelo's David revealed after clean-up. <https://www.newscientist.com/article/dn5028-michelangelo-david-revealed-after-clean-up/>. Accessed Dec 2021
6. Romero G (2020) The iron lady structure: atmospheric corrosion of the Eiffel Tower. <https://www.penspen.com/insights/the-iron-lady-structure-atmospheric-corrosion-of-the-eiffel-tower/>. Accessed Dec 2021
7. Jia R et al (2019) Microbiologically influenced corrosion and current mitigation strategies: a state of the art review. *Int Biodeterior Biodegrad* 137:42–58
8. Gaines RH (1910) Bacterial activity as a corrosive influence in the soil. *J Ind Eng Chem* 2(4):128–130
9. Cord-Ruwisch R, Widdel F (1986) Corroding iron as a hydrogen source for sulphate reduction in growing cultures of sulphate-reducing bacteria. *Appl Microbiol Biotechnol* 25(2):169–174
10. Venzlaff H et al (2013) Accelerated cathodic reaction in microbial corrosion of iron due to direct electron uptake by sulfate-reducing bacteria. *Corros Sci* 66:88–96
11. Enning D, Garrelfs J (2014) Corrosion of iron by sulfate-reducing bacteria: new views of an old problem. *Appl Environ Microbiol* 80(4):1226
12. Gu T et al (2021) Extracellular electron transfer in microbial biocorrosion. *Curr Opin Electrochem* 29:100763
13. Zhang R et al (2021) Editorial: bioleaching and biocorrosion: advances in interfacial processes. *Front Microbiol* 12:653029
14. Beech IB, Sunner J (2004) Biocorrosion: towards understanding interactions between biofilms and metals. *Curr Opin Biotechnol* 15(3):181–186
15. Chambers LD et al (2006) Modern approaches to marine anti-fouling coatings. *Surf Coat Technol* 201(6):3642–3652
16. Yin W et al (2021) Ways to control harmful biofilms: prevention, inhibition, and eradication. *Crit Rev Microbiol* 47(1):57–78
17. King RA, Miller JDA (1971) Corrosion by the sulphate-reducing bacteria. *Nature* 233(5320):491–492
18. Muyzer G, Stams AJM (2008) The ecology and biotechnology of sulphate-reducing bacteria. *Nat Rev Microbiol* 6(6):441–454
19. Černoušek T et al (2020) Microbially influenced corrosion of carbon steel in the presence of anaerobic sulphate-reducing bacteria. *Corros Eng Sci Technol* 55(2):127–137
20. Ziadi I et al (2019) Investigating the biocorrosion mechanism of 304L stainless steel in raw and treated urban wastewaters. *Eng Fail Anal* 101:342–356
21. Burstein GT et al (2004) Origins of pitting corrosion. *Corros Eng Sci Technol* 39(1):25–30

22. Eguchi K, Burnett TL, Engelberg DL (2020) X-ray tomographic characterisation of pitting corrosion in lean duplex stainless steel. *Corros Sci* 165:108406
23. Szklarska-Smialowska Z (2002) Mechanism of pit nucleation by electrical breakdown of the passive film. *Corros Sci* 44(5):1143–1149
24. Li Z et al (2021) Suppression mechanism of initial pitting corrosion of pure Zn by Li alloying. *Corros Sci* 189:109564
25. Rosenfeld IL, Marshakov IK (2013) Mechanism of crevice corrosion. *Corrosion* 20(4):115t–125t
26. Zhu D, Liu Y, Gilbert JL (2020) In vitro fretting crevice corrosion damage of CoCrMo alloys in phosphate buffered saline: debris generation, chemistry and distribution. *Acta Biomater* 114:449–459
27. Torres C, Johnsen R, Iannuzzi M (2021) Crevice corrosion of solution annealed 25Cr duplex stainless steels: effect of W on critical temperatures. *Corros Sci* 178:109053
28. Machuca LL et al (2013) Effect of oxygen and biofilms on crevice corrosion of UNS S31803 and UNS N08825 in natural seawater. *Corros Sci* 67:242–255
29. Guo N et al (2021) Marine bacteria inhibit corrosion of steel via synergistic biomineralization. *J Mater Sci Technol* 66:82–90
30. Salgar-Chaparro SJ et al (2020) Carbon steel corrosion by bacteria from failed seal rings at an offshore facility. *Sci Rep* 10(1):12287
31. Hladky K, Dawson JL (1981) The measurement of localized corrosion using electrochemical noise. *Corros Sci* 21(4):317–322
32. Ibrahim NF et al (2020) Corrosion inhibition properties of epoxy-zinc oxide nanocomposite coating on stainless steel 316L. *Solid State Phenom* 307:285–290
33. Mu J, Li YZ, Wang X (2021) Crevice corrosion behavior of X70 steel in NaCl solution with different pH. *Corros Sci* 182:109310
34. Harvey HJ et al (2020) Challenges and approaches in assessing the interplay between microorganisms and their physical micro-environments. *Comput Struct Biotechnol J* 18:2860–2866
35. Tian F et al (2020) Electrochemical corrosion behaviors and mechanism of carbon steel in the presence of acid-producing bacterium *Citrobacter farmeri* in artificial seawater. *Int Biodeterior Biodegrad* 147:104872
36. Kokilaramani S et al (2021) Microbial influenced corrosion of processing industry by re-circulating waste water and its control measures—a review. *Chemosphere* 265:129075
37. Alamri AH (2020) Localized corrosion and mitigation approach of steel materials used in oil and gas pipelines—an overview. *Eng Fail Anal* 116:104735
38. Chukwuike VI et al (2021) Copper corrosion mitigation: a new insight for fabricating a surface barrier film against chloride ion under hydrodynamic flow. *Appl Surf Sci* 555:149703
39. Ritala M et al (2000) Atomic layer deposition of oxide thin films with metal alkoxides as oxygen sources. *Science* 288(5464):319–321
40. Khan R, Ya HH, Pao W (2019) An experimental study on the erosion–corrosion performance of AISI 1018 carbon steel and AISI 304L stainless steel 90-degree elbow pipe. *Metals* 9(12):1260
41. Thakur A, Kumar A (2021) Sustainable inhibitors for corrosion mitigation in aggressive corrosive media: a comprehensive study. *J Bio Tribo Corros* 7(2):67
42. Laukkanen A et al (2020) Development and validation of coupled erosion–corrosion model for wear resistant steels in environments with varying pH. *Tribol Int* 151:106534
43. Cheung KH, Gu J-D (2007) Mechanism of hexavalent chromium detoxification by microorganisms and bioremediation application potential: a review. *Int Biodeterior Biodegrad* 59(1):8–15
44. Zhang J et al (2020) Hot corrosion behaviors of TP347H and HR3C stainless steel with KCl deposit in oxy-biomass combustion. *J Environ Manag* 263:110411
45. Lu H et al (2020) Erosion and corrosion behavior of shrouded plasma sprayed Cr₃C₂–NiCr coating. *Surf Coat Technol* 388:125534
46. Donlan RM, Costerton JW (2002) Biofilms: survival mechanisms of clinically relevant microorganisms. *Clin Microbiol Rev* 15(2):167–193
47. Muhammad MH et al (2020) Beyond risk: bacterial biofilms and their regulating approaches. *Front Microbiol* 11:928–928
48. Plakunov VK et al (2020) Biocorrosion of synthetic plastics: degradation mechanisms and methods of protection. *Microbiology* 89(6):647–659
49. Plaza G, Achal V (2020) Biosurfactants: eco-friendly and innovative biocides against biocorrosion. *Int J Mol Sci* 21(6):2152
50. Fytianos G et al (2020) Biocorrosion of concrete sewers in Greece: current practices and challenges. *Sustainability* 12(7):2638
51. Kokilaramani S et al (2020) *Bacillus megaterium*-induced biocorrosion on mild steel and the effect of *Artemisia pallens* methanolic extract as a natural corrosion inhibitor. *Arch Microbiol* 202(8):2311–2321
52. Arun D, Vimala R, Devendranath Ramkumar K (2020) Investigating the microbial-influenced corrosion of UNS S32750 stainless-steel base alloy and weld seams by biofilm-forming marine bacterium *Macrococcus equiperficus*. *Bioelectrochemistry* 135:107546
53. Ituen E et al (2020) Inhibition of acid and bio-corrosion of pipeline steel using tabersonine: experimental, DFT and molecular dynamics simulations approaches. *J Bio Tribo Corros* 6(4):118
54. Galarce C et al (2020) Dynamics of biocorrosion in copper pipes under actual drinking water conditions. *Water* 12(4):1036
55. Rochdi A et al (2014) Inhibitive properties of 2,5-bis(*n*-methylphenyl)-1,3,4-oxadiazole and biocide on corrosion, biocorrosion and scaling controls of brass in simulated cooling water. *Corros Sci* 80:442–452
56. Davidova IA et al (2012) Involvement of thermophilic archaea in the biocorrosion of oil pipelines. *Environ Microbiol* 14(7):1762–1771
57. Kairy SK et al (2016) On the electrochemical and quasi in situ corrosion response of the Q-phase (Al_xCu_yMg_zSi_w) intermetallic particle in 6xxx series aluminum alloys. *Corrosion* 73(1):87–99
58. Yuan SJ et al (2009) Surface functionalization of Cu–Ni alloys via grafting of a bactericidal polymer for inhibiting biocorrosion by *Desulfovibrio desulfuricans* in anaerobic seawater. *Biofouling* 25(2):109–125
59. Khan MM et al (2018) Recent advancements in bulk metallic glasses and their applications: a review. *Crit Rev Solid State Mater Sci* 43(3):233–268
60. Moradi M et al (2011) De-alloying of 316 stainless steel in the presence of a mixture of metal-oxidizing bacteria. *Corros Sci* 53(12):4282–4290
61. Dwivedi D, Lepkova K, Becker T (2017) Emerging surface characterization techniques for carbon steel corrosion: a critical brief review. *Proc R Soc A* 473(2199):20160852
62. Chiavari C et al (2008) Atmospheric corrosion of historical organ pipes: the influence of environment and materials. *Corros Sci* 50(9):2444–2455
63. Antony MM, Sandeep CSS, Matham MV (2021) High resolution probe for corrosion monitoring using hyper spectral imaging. *AIP Conf Proc* 2317(1):030016
64. Brandoli B et al (2021) Aircraft fuselage corrosion detection using artificial intelligence. *Sensors* 21(12):4026

65. Scott B et al (2021) Macro and microscopic visual imaging tools to investigate metal reducing bacteria in soils. *Soil Sci Soc Am J* 85(1):184–192
66. Mabrouki F et al (2009) Frictional heating model for efficient use of vibrothermography. *NDT E Int* 42(5):345–352
67. Del Grande N et al (2001) Dynamic thermal tomography for nondestructive inspection of aging aircraft. In: SPIE's 1993 international symposium on optics, imaging, and instrumentation. SPIE
68. Wu H, Lei H, Frank CY (2021) Comparison on mechanisms of high-cycle fatigue performance of structural steel exposed to urban industrial atmosphere and laboratory simulated corrosive environment based on infrared thermography. *Int J Fatigue* 145:106098
69. Vishwakarma V et al (2012) Biofilm formation and thermographic evaluation of fly ash concrete in sea water. *Concr Res Lett* 3(2):426–438
70. Bremer PJ, Geesey GG (1991) Laboratory-based model of microbiologically induced corrosion of copper. *Appl Environ Microbiol* 57(7):1956–1962
71. Nasrazadani S et al (2016) Application of Fourier transform infrared spectroscopy to study concrete degradation induced by biogenic sulfuric acid. *Mater Struct* 49(5):2025–2034
72. Binnig G, Quate CF, Gerber C (1986) Atomic force microscope. *Phys Rev Lett* 56(9):930–933
73. Li J, Lampner D (1999) In situ AFM study of pitting corrosion of Cu thin films. *Colloids Surf A* 154(1):227–237
74. Rugar D, Hansma P (1990) Atomic force microscopy. *Phys Today* 43(10):23–30
75. Wang R (2004) An AFM and XPS study of corrosion caused by micro-liquid of dilute sulfuric acid on stainless steel. *Appl Surf Sci* 227(1):399–409
76. Xu L-C, Chan K-Y, Fang HHP (2002) Application of atomic force microscopy in the study of microbiologically influenced corrosion. *Mater Charact* 48(2):195–203
77. Mu G, Li X (2005) Inhibition of cold rolled steel corrosion by Tween-20 in sulfuric acid: weight loss, electrochemical and AFM approaches. *J Colloid Interface Sci* 289(1):184–192
78. Olivares-Xometl O et al (2006) Surface analysis of inhibitor films formed by imidazolines and amides on mild steel in an acidic environment. *Appl Surf Sci* 252(6):2139–2152
79. Yuan SJ, Pehkonen SO (2009) AFM study of microbial colonization and its deleterious effect on 304 stainless steel by *Pseudomonas NCIMB 2021* and *Desulfovibrio desulfuricans* in simulated seawater. *Corros Sci* 51(6):1372–1385
80. Chen H et al (2020) Application of electrochemical atomic force microscopy (EC-AFM) in the corrosion study of metallic materials. *Materials* 13(3):668
81. Geiger SL, Ross TJ, Barton LL (1993) Environmental scanning electron microscope (ESEM) evaluation of crystal and plaque formation associated with biocorrosion. *Microsc Res Tech* 25(5–6):429–433
82. Franklin MJ, White DC (1991) Biocorrosion. *Curr Opin Biotechnol* 2(3):450–456
83. Wu Y et al (2020) Tracking the fungus-assisted biocorrosion of lead metal by Raman imaging and scanning electron microscopy technique. *J Raman Spectrosc* 51(3):508–513
84. Chapman J, Weir E, Regan F (2010) Period four metal nanoparticles on the inhibition of biofouling. *Colloids Surf B* 78(2):208–216
85. Chapman J et al (2010) Phthalate doped PVC membranes for the inhibition of fouling. *J Membr Sci* 365(1–2):180–187
86. Sullivan T, Chapman J, Regan F (2011) Characterisation of nano-antimicrobial materials. In: *Nano-antimicrobials*. Springer, Berlin, p 181–208
87. Chapman J, Regan F (2011) Sebacic and succinic acid derived plasticized PVC for the inhibition of biofouling in its initial stages. *J Appl Biomater Biomech* 9(3):176–184
88. Sullivan T, Chapman J, Regan F (2012) Characterisation of nano-antimicrobial materials. In: *Nano-antimicrobials: progress and prospects*. Springer, Berlin, p 181–208
89. Chapman J, Regan F (2012) Nanofunctionalized superhydrophobic antifouling coatings for environmental sensor applications—advancing deployment with answers from nature. *Adv Eng Mater* 14(4):8175–8184
90. Chapman J et al (2013) Antifouling performances of macro- to micro-to nano-copper materials for the inhibition of biofouling in its early stages. *J Mater Chem B* 1(45):6194–6200
91. Chapman J et al (2014) Bioinspired synthetic macroalgae: examples from nature for antifouling applications. *Int Biodeterior Biodegrad* 86:6–13
92. Gangadoo S et al (2018) Selenium nanoparticles in poultry feed modify gut microbiota and increase abundance of *Faecalibacterium prausnitzii*. *Appl Microbiol Biotechnol* 102(3):1455–1466
93. Rajapaksha P et al (2018) Graphene, electrospun membranes and granular activated carbon for eliminating heavy metals, pesticides and bacteria in water and wastewater treatment processes. *Analyst* 143(23):5629–5645
94. Zhou J et al (2020) Direct and indirect evidence of the microbially induced pitting corrosion of steel structures in humid environments. *Coatings* 10(10):983
95. Diaz B et al (2009) Electrochemical behaviour of high strength steel wires in the presence of chlorides. *Electrochim Acta* 54(22):5190–5198
96. Tsuchiya H et al (2009) Metallurgical aspects on the formation of self-organized anodic oxide nanotube layers. *Electrochim Acta* 54(22):5155–5162
97. Wang Y, Jiang Z, Yao Z (2009) Preparation and properties of ceramic coating on Q235 carbon steel by plasma electrolytic oxidation. *Curr Appl Phys* 9(5):1067–1071
98. Chang HT, Rittmann BE (1986) Biofilm loss during sample preparation for scanning electron microscopy. *Water Res* 20(11):1451–1456
99. Sutton NA, Hughes N, Handley PS (1994) A comparison of conventional SEM techniques, low temperature SEM and the electroscan wet scanning electron microscope to study the structure of a biofilm of *Streptococcus crista* CR3. *J Appl Bacteriol* 76(5):448–454
100. Little B et al (1991) Biofilms: An ESEM evaluation of artifacts introduced during SEM preparation. *J Ind Microbiol* 8(4):213–221
101. Wagner PA, Ray RI (1994). In: Kearns JR, Little BJ (eds) *Surface analytical techniques for microbiologically influenced corrosion—a review*. ASTM International, West Conshohocken, pp 153–169
102. Gregerová M, Všianský D (2009) Identification of concrete deteriorating minerals by polarizing and scanning electron microscopy. *Mater Charact* 60(7):680–685
103. Seah MP (1980) The quantitative analysis of surfaces by XPS: a review. *Surf Interface Anal* 2(6):222–239
104. Yang L, Zhang E (2009) Biocorrosion behavior of magnesium alloy in different simulated fluids for biomedical application. *Mater Sci Eng C* 29(5):1691–1696
105. Johansson L-S, Saastamoinen T (1999) Investigating early stages of biocorrosion with XPS: AISI 304 stainless steel exposed to *Burkholderia* species. *Appl Surf Sci* 144–145:244–248
106. Chen G, Palmer RJ, White DC (1997) Instrumental analysis of microbiologically influenced corrosion. *Biodegradation* 8(3):189–200
107. Juzeliūnas E et al (2007) Microbially influenced corrosion of zinc and aluminium—two-year subjection to influence of *Aspergillus niger*. *Corros Sci* 49(11):4098–4112
108. Veiga-Santos P et al (2005) Microstructure and color of starch-gum films: effect of gum deacetylation and additives. Part 2. *Food Hydrocoll* 19(6):1064–1073
109. Fang HH, Chan K-Y, Xu L-C (2000) Quantification of bacterial adhesion forces using atomic force microscopy (AFM). *J Microbiol Methods* 40(1):89–97
110. Saleem Khan M et al (2019) Microbiologically influenced corrosion of titanium caused by aerobic marine bacterium *Pseudomonas aeruginosa*. *J Mater Sci Technol* 35(1):216–222

111. Yu S et al (2020) Microbiologically influenced corrosion of 304 stainless steel by nitrate reducing *Bacillus cereus* in simulated Beijing soil solution. *Bioelectrochemistry* 133:107477
112. Reyes A et al (2008) Microbiologically induced corrosion of copper pipes in low-pH water. *Int Biodeterior Biodegrad* 61(2):135–141
113. Dinu CZ et al (2007) Monitoring nitinol alloy surface reactions for biofouling studies. *Appl Surf Sci* 253(19):7719–7723
114. Gebert A et al (2009) Passivity of polycrystalline NiMnGa alloys for magnetic shape memory applications. *Corros Sci* 51(5):1163–1171
115. Cardona IC, Márquez MA (2009) Biodesulfurization of two Colombian coals with native microorganisms. *Fuel Process Technol* 90(9):1099–1106
116. Calle GR et al (2007) Enhanced copper release from pipes by alternating stagnation and flow events. *Environ Sci Technol* 41(21):7430–7436
117. Kiani Khouzani M et al (2019) Microbiologically influenced corrosion of a pipeline in a petrochemical plant. *Metals* 9(4):459
118. Khanfar HS, Sitepu H (2021) Lab case study of microbiologically influenced corrosion and Rietveld quantitative phase analysis of X-ray powder diffraction data of deposits from a refinery. *ACS Omega* 6(18):11822–11831
119. Beech IB, Gaylarde CC (1999) Recent advances in the study of biocorrosion: an overview. *Rev Microbiol* 30:117–190
120. Videla HA (2002) Prevention and control of biocorrosion. *Int Biodeterior Biodegrad* 49(4):259–270
121. Mansfeld F, Oldham KB (1971) A modification of the Stern-Geary linear polarization equation. *Corros Sci* 11(10):787–796
122. Barranco V, Feliu S, Feliu S (2004) EIS study of the corrosion behaviour of zinc-based coatings on steel in quiescent 3% NaCl solution. Part 1: directly exposed coatings. *Corros Sci* 46(9):2203–2220
123. Videla HA, Herrera LK (2004) Chapter 7: biocorrosion. In: Vazquez-Duhalt R, Quintero-Ramirez R (eds) *Studies in surface science and catalysis*. Elsevier, Amsterdam, pp 193–218
124. Agarwala VS, Reed PL, Ahmad S (2000) Corrosion detection and monitoring—a review. In: *CORROSION 2000*
125. Mehrazi S, Saremi M, Neshati J (2016) A probe into low-temperature stress corrosion cracking of 304L stainless steel by scanning vibrating electrode technique. *Corros Eng Sci Technol* 51(5):358–364
126. Chelliah NM, Padaikathan P, Kumar R (2019) Evaluation of electrochemical impedance and biocorrosion characteristics of as-cast and T4 heat treated AZ91 Mg-alloys in Ringer's solution. *J Magnes Alloys* 7(1):134–143
127. Miranda E et al (2006) Biocorrosion of carbon steel alloys by an hydrogenotrophic sulfate-reducing bacterium *Desulfovibrio capillatus* isolated from a Mexican oil field separator. *Corros Sci* 48(9):2417–2431
128. Guo J et al (2009) Weather resistance of low carbon high performance bridge steel. *Mater Des* 30(1):129–134
129. Wenger F et al (1997) Electrochemical impedance of pits. Influence of the pit morphology. *Corros Sci* 39(7):1239–1252
130. Gabrielli C et al (2008) Single pit on iron generated by SECM: an electrochemical impedance spectroscopy investigation. *Electrochim Acta* 53(25):7539–7548
131. Ramírez-Platas M et al (2021) Fractal and multifractal analysis of electrochemical noise to corrosion evaluation in A36 steel and AISI 304 stainless steel exposed to MEA-CO₂ aqueous solutions. *Chaos Solitons Fractals* 145:110802
132. Finšgar M (2020) Electrochemical, 3D topography, XPS, and ToF-SIMS analyses of 4-methyl-2-phenylimidazole as a corrosion inhibitor for brass. *Corros Sci* 169:108632
133. Acosta G et al (2020) Effect of laminar flow on the corrosion activity of AA6061-T6 in seawater. *Metals* 10(2):175
134. Caldona EB, Smith DW Jr, Wipf DO (2021) Surface electro-analytical approaches to organic polymeric coatings. *Polym Int* 70(7):927–937
135. San-Blas E et al (2012) Characterization of *Xenorhabdus* and *Photorhabdus* bacteria by Fourier transform mid-infrared spectroscopy with attenuated total reflection (FT-IR/ATR). *Spectrochim Acta A* 93:58–62
136. Janbu AO et al (2008) FT-IR microspectroscopy: a promising method for the rapid identification of *Listeria* species. *FEMS Microbiol Lett* 278(2):164–170
137. Schmitt J, Flemming H-C (1998) FTIR-spectroscopy in microbial and material analysis. *Int Biodeterior Biodegrad* 41(1):1–11
138. Chapman J et al (2021) A high-throughput and machine learning resistance monitoring system to determine the point of resistance for *Escherichia coli* with tetracycline: combining UV-visible spectrophotometry with principal component analysis. *Biotechnol Bioeng* 118(4):1511–1519
139. Truong VK, Chapman J, Cozzolino D (2021) Monitoring the bacterial response to antibiotic and time growth using near-infrared spectroscopy combined with machine learning. *Food Anal Methods* 14(7):1–8
140. Cheeseman S, Shaw Z, Vongsvivut J, Crawford RJ, Dupont MF, Boyce K, Gangadoo S, Owen S, Bryant SJ, Bryant G, Cozzolino D, Chapman J, Elbourne A, Truong VK (2021) Analysis of pathogenic bacterial and fungal biofilms using the combination of synchrotron ATR-FTIR microspectroscopy and chemometric approaches. *Molecules* 26(13):3890. <https://doi.org/10.3390/molecules26133890>
141. Pham DQ, Bryant SJ, Cheeseman S, Huang LZ, Bryant G, Dupont MF, Chapman J, Berndt CC, Vongsvivut J, Crawford RJ, Truong VK, Ang ASM, Elbourne A (2020) Micro- to nano-scale chemical and mechanical mapping of antimicrobial-resistant fungal biofilms. *Nanoscale* 12:19888–19904. <https://doi.org/10.1039/D0NR05617K>
142. Salaita GN (1995) Determination of the spatial distribution of trace elements in stainless steel by imaging microprobe secondary ion mass spectrometry. *Appl Surf Sci* 90(4):465–479
143. Hasan N, Gopal J, Wu HF (2011) Rapid, sensitive and direct analysis of exopolysaccharides from biofilm on aluminum surfaces exposed to sea water using MALDI-TOF MS. *J Mass Spectrom* 46(11):1160–1167
144. Beale D et al (2017) A community multi-omics approach towards the assessment of surface water quality in an urban river system. *Int J Environ Res Public Health* 14(3):303
145. McDonnell LA, Heeren RM (2007) Imaging mass spectrometry. *Mass Spectrom Rev* 26(4):606–643
146. Brauer JI et al (2017) Metabolomic imaging of a quaternary ammonium salt within a marine bacterial biofilm on carbon steel. *Int Biodeterior Biodegrad* 125:33–36
147. Kotu SP, Mannan MS, Jayaraman A (2019) Emerging molecular techniques for studying microbial community composition and function in microbiologically influenced corrosion. *Int Biodeterior Biodegrad* 144:104722